Soft Wearable Body-Powered Hydraulic Actuation System for a Prosthetic Finger Design

Kamyar Motaghedolhagh*, Azadeh Shariati*, Shervanthi Homer-Vanniasinkam, Helge A Wurdemann

***Abstract*— Objective: Finger and fingertip loss is the most common form of upper-limb amputation. With a focus on amputations involving the loss of distal and/or partial middle finger segments, this paper outlines the design and development of a novel soft body-powered hydraulically-driven actuation system for a prosthetic finger, while offering an in-depth examination of its subsystems. Method: The proposed device utilises a soft wearable hydraulic mechanism to transfer pressure from the proximal interphalangeal (PIP) joint of the human finger to the distal interphalangeal (DIP) joint of the prosthetic finger, enabling movement of the soft prosthetic DIP joint. The design parameters of the soft actuator, such as its configuration, constituent material, and volume were analysed through experiments with able-bodied participants. Each participant tried 42 different actuators while flexing their index finger, repeating the task four times, yielding 168 trials per participant. The human and prosthetic finger flexion angles and resultant pressures were measured using an Aurora electromagnetic sensor and a fluid pressure transducer. All data was segmented and analysed. Result: Soft actuator designs were selected through statistical analysis of the material (Agilus 30 and Dragon Skin 30), configuration (chambers located underside or around the PIP joint), and volume. Conclusion: The study demonstrated that the selected soft wearable hydraulic mechanism transferred generated pressure from the participant's PIP joint effectively, enabling movement of the prosthetic digit. Significance: Our research contributes to current developments in versatile body-powered prosthetic devices, laying the foundations for broad applications in affordable healthcare devices.**

***Index Terms*— Body-powered prosthetic finger, Hydraulically-driven, Distal interphalangeal joint, Proximal interphalangeal joint, Soft actuator, Wearable mechanism.**

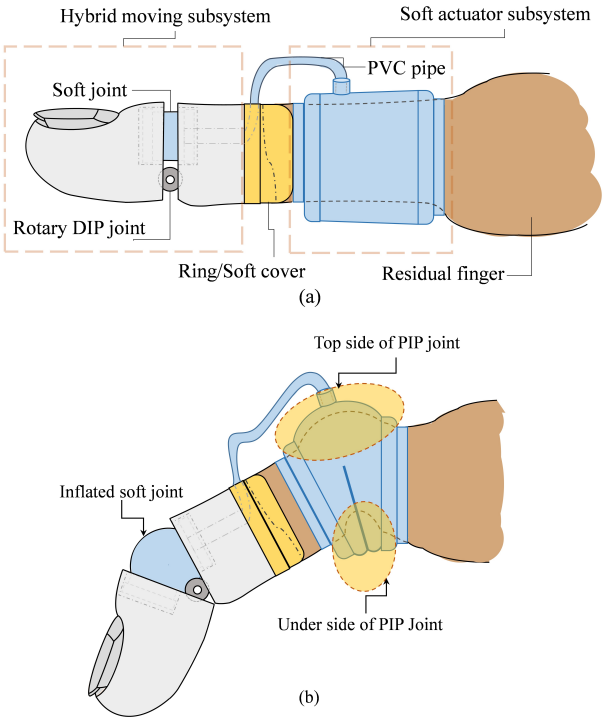

Fig. 1. Representation of the body-powered prosthetic finger concept, featuring two main subsystems connected by a PVC pipe connector: the soft actuator subsystem and the hybrid moving subsystem. (a) Unactuated prosthetic finger. (b) Actuated prosthetic finger, demonstrating fluid transmission from the PIP to the DIP soft joint, enabling DIP joint flexion during amputee finger movement.

I. Introduction

FINGER and fingertip amputation accounts for 86% of all upper-limb amputations globally [1]. Around 0.4% of the US population have experienced upper or lower limb amputation, while the incidence rate is 50,000 new cases per year [2]. One in four amputations are upper limb related, and, in developing countries, 80% of these cases are a consequence of scarring, deformity, and dysfunction caused by external trauma. In developed nations, the disease accounts for 68% of limb amputations, while trauma-related amputations represent approximately 30%, and congenital limb deformities up to 3% [3]. Young men have a heightened likelihood of experiencing amputation due to traumatic injuries, particularly those related to motor vehicle accidents or to machinery in the workplace [4]. A significant proportion of forearm amputees, 60%, fall within the age range of 21-64, while 10% are under 21 years old [5]. The impact of finger and fingertip amputation on patients extends beyond physical inconvenience, with negative effects on mental health. Kearns et al. found that nearly one-third of patients with partial-hand amputations screened positive for Post-Traumatic Stress Disorder (PTSD) [6]. They

*This work is supported by the Springboard Award of the Academy of Medical Sciences (grant number: SBF003-1109), and the Engineering and Physical Sciences Research Council (grant numbers: EP/R037795/1, EP/S014039/1, and EP/V01062X/1).

K. Motaghedolhagh, A. Shariati, and H. Wurdemann are with the Department of Mechanical Engineering, University College London, WC1E 7JE, UK. k.motagedolhagh@ucl.ac.uk, a.shariati@ucl.ac.uk, h.wurdemann@ucl.ac.uk S.H. Homer-Vanniasinkam is with the Multiscale Cardiovascular Engineering Group, University College London, WC1E 7JE, UK. s.homer-v@ucl.ac.uk (*Kamyar Motaghedolhagh and Azadeh Shariati contributed equally to this work.)

investigated the relationship between different levels of limb loss (partial hand vs. higher levels) and psychological well-being. Their findings revealed that individuals with partial hand loss are more likely to experience pain and screen positive for PTSD, as compared to those with higher levels of limb loss. Emotional reactions were also seen to vary significantly based on the level of limb loss; those participants with partial hand loss reported greater emotional distress [6]. Prosthetic fingers can restore some degree of hand function and improve quality of life. For patients with well-preserved residual fingers, problems can be overcome through micro-surgical (vascular) reconstruction [7]. However, in cases where patients have had a more significant amputation or have undergone unsuccessful surgery, prostheses can improve functionality [8]. Surgically fusing the DIP joint at specific angles (0, 15, or 25 degrees) is a recognised method in cases where reconstructive methods are not applicable [9]. However, restoring the finger's natural anatomy with an active DIP joint is the preferred route as it leads to improved functionality and grip strength, enabling patients to participate in a wider range of activities [10].

A variety of prosthetic options are available for finger and fingertip rehabilitation. **Passive functional prostheses** offer no intrinsic active motion but can facilitate holding or grasping objects and in the performance of other simple tasks [11], [12]. **Activity-specific prostheses** are designed to enable the performance of specific tasks such as grasping an object, applying pressure to a specific object, or throwing [13]–[16]. **Externally-powered prostheses** are driven by electric motors, and enable amputees to perform a range of finger and hand movements [17]–[20]. **Body-powered prostheses** are devices that capture body motion to affect functionality in specific tasks [21]–[25].

These types of prostheses can be categorised into three groups, based on their actuation systems: **cable-operated prostheses,** in which specific body motions control the cables resulting in prosthetic movement; [26]; **implant-operated prostheses,** which are activated by muscle contractions in the residual limb [27]–[29]; and **residual-finger- or limb-operated prostheses,** which are activated by the remaining fingers or residual limbs [30].

A variety of actuation methods and mechanisms are employed to operate prosthetic fingers [31]. One potential but rarely explored actuation mechanism involves the utilisation of hydraulic or pneumatic systems. Although some progress has recently been made in the development of externally-powered prostheses using pneumatic actuation, there appears to have been no research into hydraulically/pneumatically actuated body-powered prosthetic devices [32]. In relation to externally-powered fingers using hydraulic actuation, Takamaya et al. developed a three-fingered retractor hand with hydraulic-driven bending joints, that aimed at simplifying the mechanism and enhancing safety during retraction. The design ensured balanced fingertip forces, adjustable load torque for finger extension through precompression modification, and adaptable compliance leveraging the elasticity of tubes within the hydraulic joints [33]. In relation to externally-powered prostheses utilising pneumatic actuation, Gu et al. developed an innovative neuro-prosthetic hand with six active degrees of freedom (DoF), each soft finger being pneumatically actuated to provide flexion, while supplemented by a thumb-palm connection for additional circumduction DoF. They opted for pneumatically actuated soft fingers on account of their cost-effectiveness, lightweight nature, and ease of fabrication at scale [34]. Devi et al. investigated the use of a flexible rubber-based asymmetric bellow bending joint. This was done during the development of a soft robotic hand with multiple joints and fingers for prosthetic applications. Their proposed joint, with its single internal chamber, offered simplicity, compactness, and ease of manufacture [35].

Body-powered prostheses have several advantages. Unlike externally-powered prosthetic devices, they have the ability to convey force feedback to amputees, a desirable feature for amputees [36]. Force feedback enhances user performance, as demonstrated by Gonzalas et al., who found that accuracy in delicate task performance is highest when visual and force feedback is combined, followed by force feedback alone, followed by visual feedback alone [36]. Typically, body-powered prostheses are also lightweight, cheaper to manufacture and maintain, more durable, and capable of functioning effectively under various environmental conditions. [37].

An innovative body-powered hydraulically-driven prosthetic finger made of soft wearable components is presented in this study. It is based on the premise that soft DIP joints on prosthetic fingers can be bent without external power - the actuation energy being harvested from the PIP joint. Our device was fabricated and then evaluated through an experiment with able-bodied participants. The pressure generated by the soft actuator and the flexion angles of both the participant's PIP joint and the prosthetic finger's DIP joint were quantified. Various configurations, volumes, and constituent materials of the soft actuator were also investigated to determine their effects on the prosthetic device's performance. The key contributions of this study are as follows:

- The development and assessment of an innovative design for hydraulically driven body-powered finger prostheses. The design incorporates a hydraulic soft actuator instead of conventional rigid mechanisms.
- The experimental determination of design parameters for the hydraulic soft actuator in terms of volume, configuration, and constituent material, as evaluated through testing with able-bodied participants. The findings from these experiments provide insights into the actuator's performance characteristics and its wider potential applications.

The structure of this paper is as follows: Section II outlines the concept of the prosthetic finger based on certain design assumptions. Section III describes the design and fabrication process of the proposed wearable body-powered prosthetic finger. Section IV details the experimental setup, hardware architecture, and protocol utilised to evaluate the device's functionality and performance. Section V covers data capture and segmentation. Section VI presents experimental results, statistically analysed. Section VII considers the selection of the most suitable soft actuation subsystem, while limitations and potential future work are presented in Section VIII. Finally, in Section IX, we summarise the overall research conclusions

and outcomes.

II. Concept Overview of the Prosthetic Finger

Figure 1 illustrates the design of our novel prosthetic finger. A soft actuator on the PIP joint of the human finger generates the fluid pressure necessary to move the soft DIP joint of the prosthetic finger. The adopted assumptions and conditions that underlie the design are as follows:

- The prosthetic finger is for individuals who have lost either just the distal phalange or the distal along with a section of the middle phalange, of their index fingers. It can also be adapted for use on other fingers though not for the thumb.
- The proposed finger prosthesis is purely mechanically driven and does not use external electrical power or electromyography (EMG) signals.
- The finger prosthesis is non-implanted.
- Unlike most body-powered prosthetic fingers, it does not require ancillary parts such as a wrist strap or glove - indeed the prosthesis can be simply attached to the amputee's finger using a cover or a ring.

The proposed body-powered prosthetic digit has two main subsystems: the soft actuator subsystem and the hybrid moving subsystem.

A. Soft actuator subsystem

The soft actuator subsystem is a hydro-mechanical device that uses fluids, such as water or oil, to transmit pressure. The fluid is held within a soft container that surrounds the PIP joint of the human finger. As seen in Fig. 1(b), when amputees bend their PIP joint, the two main spaces above and below work together to generate and harness the necessary energy to bend the prosthetic finger's DIP joint.

B. Hybrid moving subsystem

The hybrid moving subsystem comprises two rigid segments connected by a rotary joint and a soft silicone chamber. Fig. 1(a) illustrates the unactuated finger prosthesis while Fig. 1(b) shows it actuated. Altering the fluid volume in the soft actuator leads to joint flexion of the prosthetic finger's DIP. When the amputee flexes the residual finger's PIP joint, the fluid volume in the soft actuator decreases, as it pushes fluid through a small PVC pipe to the DIP joint of the prosthetic finger. This movement results in an increase in fluid volume, and therefore inflation in the soft joint, causing flexion of the prosthetic finger's DIP joint. Conversely, when the amputee straightens the PIP joint, the soft actuator returns to its original shape, the surplus fluid in the soft joint returning to the actuator and causing the DIP joint to straighten.

III. Design and Fabrication Method

A. Soft actuator subsystem

Three distinct designs of the soft actuator were developed, with each design then fabricated using three different soft materials - Ecoflex 00-50, Dragon Skin 30, and Agilus 30

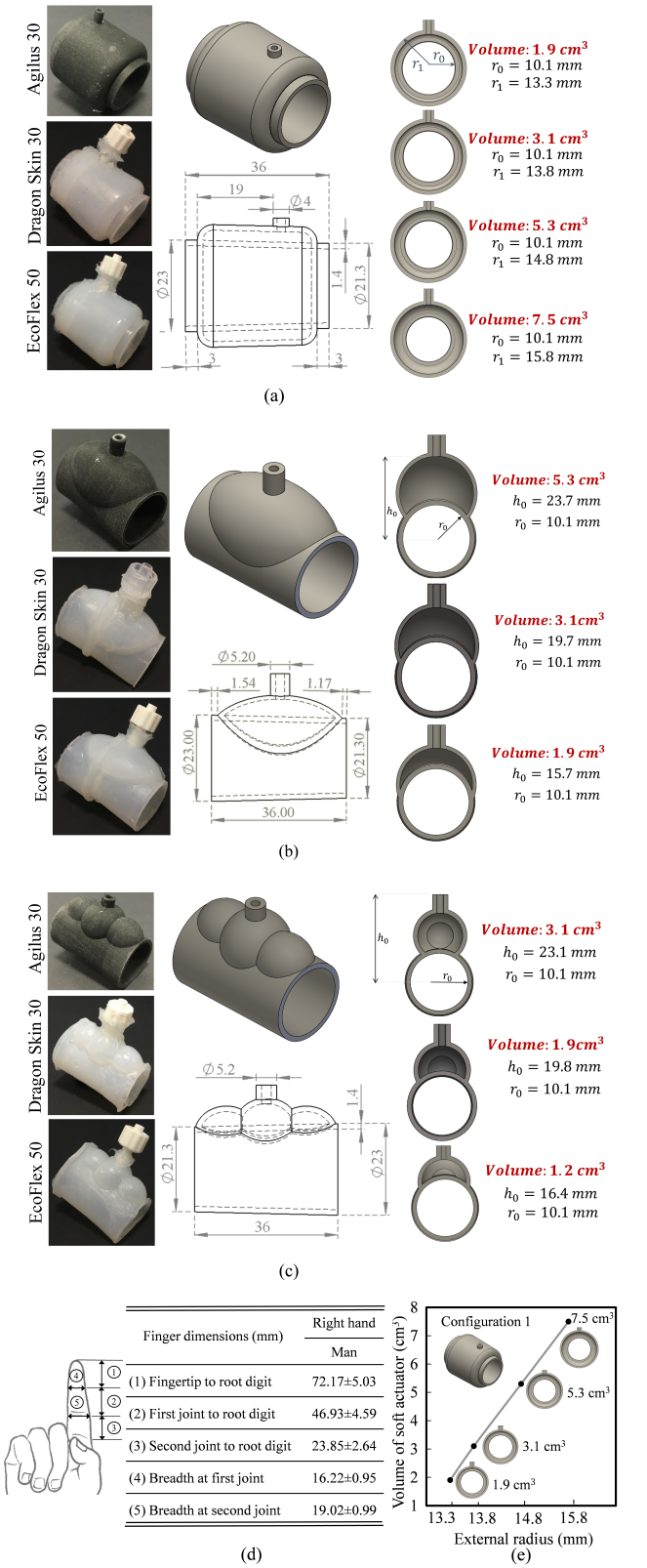

Fig. 2. Soft actuators utilised in the study. (a) Configuration 1: Actuator surrounds the PIP joint of the human finger. (b) Configurations 2 and 4: single bellow chamber located on the topside or underside of the PIP joint. (c) Configurations 3 and 5: Triple bellow chamber located on the topside or underside of the PIP joint. (d) Men's right-hand index finger dimensions [38]. (e) The annular volume of soft actuators versus the outer radius for Configuration 1.

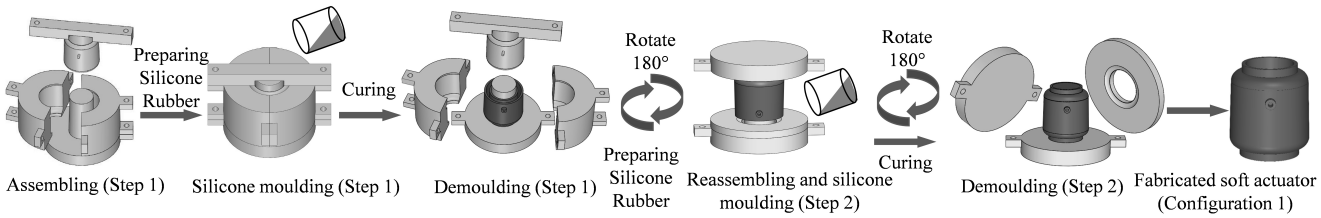

Fig. 3. The moulding process for producing a soft actuator subsystem (Configuration 1) involves two steps. In step 1, the main body of the soft actuator is created, but the fluid chamber remains open. In step 2, the fluid chamber is sealed by reassembling and applying silicone moulding. For other configurations, these steps are replicated using different moulds.

- as illustrated in Fig. 2. Table I outlines the mechanical specifications of these soft materials. For each design/material configuration, we also varied their capacities to evaluate the effect of fluid volume on actuator performance. Configurations 1 through 5 can be categorised as follows:

- Configuration 1: As illustrated in Fig. 2(a), the fluid chamber in this configuration encases the entire area around the PIP joint of the human finger, utilising the pressure differential generated around the joint. In total, we made 10 different models: Agilus 30 (with volumes of 1.9 cm^3, 3.1 cm^3, 5.3 cm^3 and 7.5 cm^3), Dragon Skin 30 (with volumes of 1.9 cm^3, 3.1 cm^3, and 5.3 cm^3), and Ecoflex 00-50 (with a volume of 1.9 cm^3, 3.1 cm^3, and 5.3 cm^3).
- Configuration 2: As shown in Fig. 2(b), this configuration consists of a semi-ellipsoid chamber on one side of the actuator cover. In this configuration, the single bellow chamber is located above the human PIP joint. In total, we made 7 different models: Agilus 30 (with volumes of 1.9 cm^3, 3.1 cm^3, and 5.3 cm^3), Dragon Skin 30 (with a volume of 1.9 cm^3, 3.1 cm^3), and Ecoflex 00-50 (with a volume of 1.9 cm^3, 3.1 cm^3).
- Configuration 3: Shaped differently from Configuration 2, this triple bellow chamber can also be located above the PIP joint to utilise the generated pressures. In total, we made 9 different models: Agilus 30 (with volumes of 1.2 cm^3, 1.9 cm^3, and 3.1 cm^3), Dragon Skin 30 (with a volume of 1.2 cm^3, 1.9 cm^3, and 3.1 cm^3), and Ecoflex 00-50 (with a volume of 1.2 cm^3, 1.9 cm^3, and 3.1 cm^3) - see Fig. 2(c).
- Configuration 4: This configuration is as per Configuration 2, though the semi-ellipsoid chamber is located on the underside of the human PIP joint, to utilise the generated pressure below the joint.
- Configurations 5: This configuration is as per Configuration 3, though the triple chamber is located on the underside of the human PIP joint, to utilise the generated pressure below the joint.

Due to the relatively simple shape of Configuration 1, we used this version to determine the various sizes/volumes. Having established the typical cross-sectional diameter of a man's index finger PIP joint to be 19.02±0.99 mm [38] (see Fig. 2(d)), we selected an inner diameter of 20.2 mm for all our soft actuators, so as to accommodate both women's and men's fingers. Initially, we worked on an outer radius of 13.3 mm, resulting in an annular volume of 1.9 cm^3. To produce actuators with different volumes, we parametrically increased the outer radii by 0.5 mm, 1 mm, and 2 mm, resulting in volumes of 3.1 cm^3, 5.3 cm^3, and 7.5 cm^3, respectively. The annular volumes were obtained taking into account the conical frustum shape of the actuators. As depicted in Fig. 2(e), there is a linear relationship between outer radius and volume.

In Configurations 2 and 3, the dimensions were adjusted to obtain volumes equal to those in Configuration 1. High volumes (7.5 cm^3 in Configuration 2) and (5.3 cm^3 and 7.5 cm^3 in Configuration 3) needed a very large bellow and were therefore disregarded for aesthetic reasons. We designed a low volume option (1.2 cm^3) for Configuration 3, so as to have three distinct versions of this configuration. All subsystems were designed using Solidworks software (SolidWorks, 2021, Licensed by UCL, Santa Monica, CA, USA).

The maximum outer diameter of the soft actuator was determined based on the natural position of the hand. In this position, the fingers are slightly curved or flexed, with a small gap between each finger. This arrangement provides comfort and flexibility while maintaining a natural resting posture. Yang et al. examined the preferred hand posture that users feel facilitates button pressing, estimating that the Euclidean distance between the index and middle fingertip is between 30 and 33 mm [39]. Taking into account average hand geometry [39] and the findings from Yang's study [38], we determined that the gap between the index and middle finger near the PIP joint position is around 6 mm. As a consequence, we restricted the width of our actuators to 6 mm. As illustrated in Fig. 2(a), the largest of the actuators (in Configuration 1) has an inner radius of 10.1 mm and an outer radius of 15.8 mm, and therefore a width of 5.7mm, just shy of the 6 mm limit. The hydraulic chambers in actuators 2 to 5 are positioned either above or below the PIP joint and so do not present any issues

TABLE I
MECHANICAL SPECIFICATION OF SOFT MATERIALS

Material	Specific Gravity $[gr/cm^3]$	Tensile Strength $[psi]$	Elongation at break [%]
Ecoflex $00-30^*$	1.07	200	900
Ecoflex $00-50^{**}$	1.07	315	980
Dragon Skin 30^{**}	1.08	500	364
Agilus 30^{**}	1.14	$348-450$	$220-270$

* Ecoflex 00-30 used in the soft joint fabrication.
** Ecoflex 00-50, Dragon Skin 30, and Agilus 30 were used in the soft actuator fabrication.

in this regard.

Marechal et al. catalogued the properties of a wide set of commercially available hyperelastic materials that are commonly used in soft robotics [40]. Among these materials, the Dragon Skin Series generally stands out with relatively high tensile strength at break, reaching up to 35 MPa for Dragon Skin 30. Manschot estimated the tensile strength of human skin to be 4.6–20 Mpa (652-2900 psi) [41], [42]. Materials with higher tensile strength could result in user discomfort, so Dragon Skin 30 was chosen as its tensile strength is close to, but slightly lower than that of human skin. We explored alternative additive manufacturing options, including Ecoflex 00-50, which offers reasonable tensile strength alongside nearly twice as much stretch as Dragon Skin 30, and Agilus 30, whose tensile strength falls within the range of 348-450 psi, which is lower than that of Dragon Skin 30 but higher than that of Ecoflex 00-50. Overall, these silicone-based materials exhibit the longest shelf life among mould rubbers and are commonly used in the production of medical prosthetic and orthotic devices. They are also certified as skin-safe, making them suitable for direct application onto human skin [Smooth-on Inc., USA].

Among the various methods of manufacturing soft actuators [43], two were selected that met the requirement of precision fabricating a closed soft chamber to within 1 mm. These were gravity moulding and Polyjet 3D printing. We utilised the latest technology in multi-material additive manufacturing (Stratasys J835 prints in a high mix mode), allowing 3D printing of flexible, rubber-like materials. The moulding process was also used to fabricate soft rubber joints, while the rigid parts of the finger (Clear Resin) were 3D printed. Table I shows the mechanical property specifications of the various soft materials. Because the closed chambers in the soft actuators require fluid filling, a one-step moulding process is not suitable for fabrication. It requires three steps: assembling, silicone moulding, and demoulding. The process, which is essentially the same for each configuration, is outlined in Fig. 3, which uses Configuration 1 as an illustration. Silicone materials are initially placed in a vacuum chamber to remove any bubbles. The materials are then poured into the mould at room temperature and left to cure for 4 to 6 hours. Using high temperatures in an oven can expedite the curing process without affecting material property specifications and indeed this approach has previously been used in the fabrication of soft actuators. The Agilus 30 actuators were manufactured using a Polyjet 3D printing process capable of creating soft empty chambers (www.stratasys.com). The support material removal is facilitated by a solvent, which dissolves the supporting parts within a closed chamber, before being extracted through a small opening. It typically takes 3-7 days for the solvent to fully dissolve the supports within the actuator. While other 3D printing methods, including Stereolithography, were considered for the fabrication of soft actuators, they were deemed unsuitable as the materials compatible with this printing method, such as Flexible 80A and Elastic 50A (www.formlabs.com), offered only limited elongation at break.

B. Hybrid moving subsystem

The hybrid moving subsystem is depicted in Fig. 4. It comprises two rigid segments, representing the distal and middle finger segments of the finger prosthesis, connected by a soft joint. This has a rotary joint and a mini chamber made of soft material. It enables the finger prosthesis to bend when the soft actuator is pressurised by the user and allows the finger prosthesis to return to a straight position when the actuator is not pressurised (i.e. when the PIP joint is in a straight position). The soft silicone chamber has a cylindrical shape made of soft material with a radius of 5 mm and a height of 10 mm. A 6 mm channel has been incorporated into the middle phalange of the prosthetic finger to accommodate the PVC connector pipe. The rigid segments were fabricated using clear resin and 3D-printing technology, while the soft joint was moulded using Ecoflex 00-30.

IV. Experimental Setup and Protocol

Selection of the ideal soft actuator was aided by experimental work with able-bodied participants. Our multi-factorial approach enabled a comprehensive study of system performance and provided insights into optimal design and material selection.

A. Participants

Ten able-bodied participants comprising 3 females and 7 males from different ethnic backgrounds took part in this study. The female and male age mean values and standard deviations were 34 ± 5 and 28 ± 4.5 years, respectively. All participants could move their fingers normally and had no known abnormalities or injuries to their fingers and hands. All participants had given written informed consent and the study had been approved by UCL's Research Ethics Committee (under application number 12453/001).

B. Hardware architecture

As shown in Fig. 5, a test stand was manufactured using aluminum profiles. NDI Aurora electromagnetic sensors were used to measure flexion angles. The Aurora system has four electromagnetic trackers, three of which are attached to the participant's hand in an aligned configuration. The fourth tracker is affixed to the distal phalanges of the finger prosthesis. The system's position and orientation tracking errors are

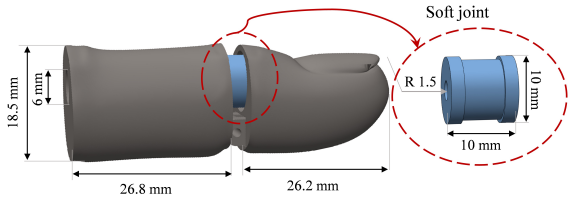

Fig. 4. The hybrid moving subsystem: Two rigid parts representing the first and the middle finger segments of the finger prosthesis connected by a soft joint linked to a soft actuator for segment flexion and return, responsive to pressure on the amputee's PIP joint.

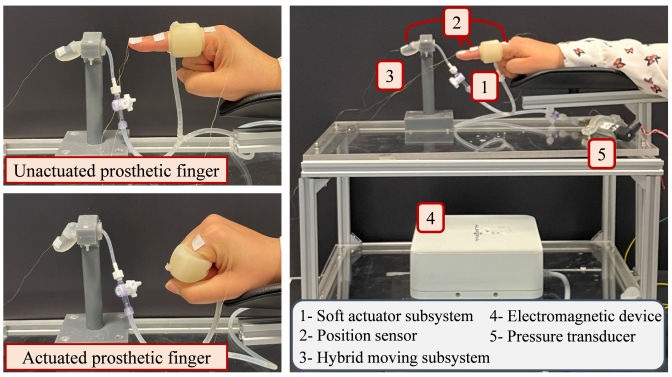

Fig. 5. Experimental setup. The hybrid moving subsystem is mounted on a fixed stand and the soft actuator subsystem is worn by the participant. To conduct the experiment, all fingers except for the index finger are initially closed (unactuated), and the index finger is closed at the end (actuated position).

less than 0.48 mm and 0.30°, respectively [44]. The generated pressure in the participant's PIP joint was measured by a fluid pressure transducer (OMEGA's PXM309) with static accuracy of ±0.25% Full Scale Best Straight Line (BSL) at 25ºC, and a National Instrument USB-6341 DAQ device was used for data acquisition.

C. Experimental protocol

Participants were given soft actuators to wear on the PIP joint of their dominant hand's index finger. They were then instructed to bend their fingers above the electromagnetic field created by the NDI Aurora system (see Fig. 5). In total each participant tested 42 actuators with different configurations, constituent materials, and volumes, as illustrated in Table IV (a Complete Block Design). The experiment time for each participant took just under 90 minutes.

1) Actuator material: To compare soft actuator materials from our selected alternatives of Ecoflex 00-50, Dragon Skin 30, and Agilus 30, we fabricated soft actuators from each material while maintaining consistent volumes for each configuration.

2) Actuator volume: To select a volume from the 1.2, 1.9, 3.1, 5.3, and 7.5 cm^3 options, we constructed soft actuators using the same material.

3) Configuration of soft actuator: To select the configuration, we constructed soft actuators, again using the same material and the same volume.

TABLE II
ACTUATORS SPECIFICATIONS. MATERIALS, VOLUMES, AND CONFIGURATION OF 42 FABRICATED SOFT ACTUATORS

Shape	Material	Volume (cm^3)				
		1.2	1.9	3.1	5.3	7.5
Configuration 1	Ecoflex 00-50		1*	2	3	
	Dragon Skin 30		4	5	6	
	Agilus 30		7	8	9	10
Configuration 2	Ecoflex 00-50		11	12		
	Dragon Skin 30		13	14		
	Agilus 30		15	16	17	
Configuration 3	Ecoflex 00-50	18	19	20		
	Dragon Skin 30	21	22	23		
	Agilus 30	24	25	26		
Configuration 4	Ecoflex 00-50		27	28		
	Dragon Skin 30		29	30		
	Agilus 30		31	32	33	
Configuration 5	Ecoflex 00-50	34	35	36		
	Dragon Skin 30	37	38	39		
	Agilus 30	40	41	42		

* Identifying numbers for soft actuators.

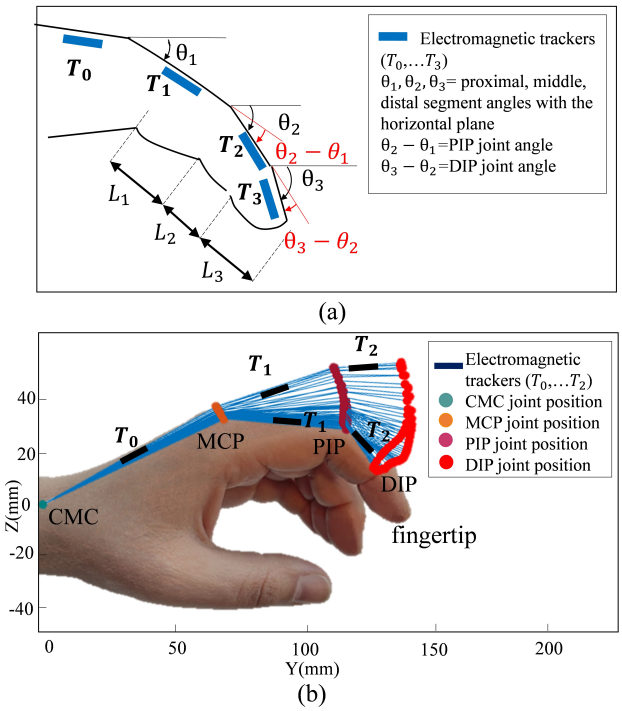

Fig. 6. (a) The positions and finger segment's angles measured by Aurora trackers (b) Representation of DIP, PIP, MCP, and CMC joints' positions of a participant captured by three NDI Aurora Electromagnetic trackers.

D. Statistical Analysis Method

We employed three-way ANOVA followed by Tukey's post-hoc test in JMP Pro 17.0 software to evaluate interactions among independent variables. The varying independent variables included the material (Ecoflex 00-50, Dragon Skin 30, and Agilus 30), volume (1.9 and 3.1 cm³), and configuration (Configurations 1 to 5). The dependent variables were generated pressures and prosthetic finger's DIP joint flexion angles.

E. Fingertip Force

We examined the fingertip force exerted by a selection of actuators to ascertain their appropriateness for fine motor tasks. Our experimental setup, depicted in Fig. 9(d), included a force measurement system comprising a six-axis force/torque sensor (IIT FT17) with a sensitivity of 0.318 mN, mounted on a linear rail (Zaber X LSM100A).

V. DATA CAPTURING AND DATA SEGMENTATION

The NDI Aurora Electromagnetic tracking system provides us with a method of capturing finger movement. Three trackers

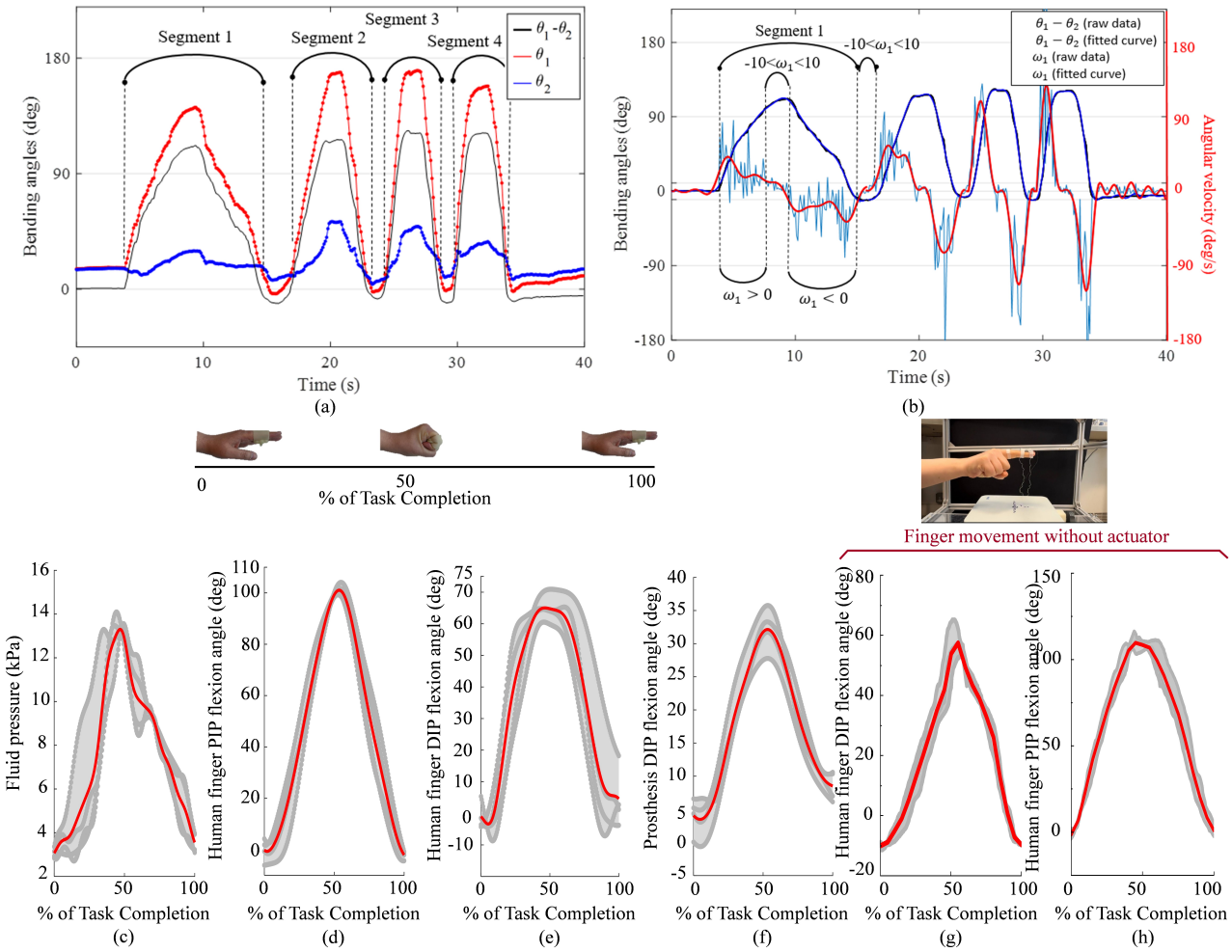

Fig. 7. (a) Angle between the middle segment of a participant's finger and horizontal plane ($\boldsymbol{\theta_1}$), the angle between proximal segment of a participant's finger and horizontal plane ($\boldsymbol{\theta_2}$), and the flexion angle between middle and proximal segments ($\boldsymbol{\theta_1 - \theta_2}$). (b) Flexion angle i.e. $\boldsymbol{\theta_1 - \theta_2}$, raw data and fitted curves, angular velocity $\boldsymbol{\omega_1}$ (a derivative of $\boldsymbol{\theta_1 - \theta_2}$) for both raw data and fitted curve. (c) Fluid pressure versus task completion (data per segment is normalised and depicted vs. task completion). (d) Human PIP flexion versus task completion. (e) Human DIP flexion versus task completion, and (f) Prosthesis DIP flexion versus task completion. (g) Human DIP flexion vs. task completion (without wearing a soft actuator). (h) Human PIP flexion vs. task completion (without wearing a soft actuator). The gray lines show segments and the red lines show the mean values. These graphs are for one participant per task.

(Fig. 6) are placed on the middle, proximal, and metacarpal segments of the participant's finger. They measure the MCP and PIP joints' flexion angles and DIP, PIP, and MCP positions. Alternatively, the three trackers can be attached to the distal, middle, and proximal segments to monitor the DIP and PIP angles and the DIP, PIP, and tip positions of the finger. Each electromagnetic tracker has five Degrees-of-Freedom including three positions in the universal coordinates x_i, y_i, z_i and two angles θ_{xi} and θ_{y_i}, ($i = 1, .., 4$ for 4 trackers). The origin of the universal coordinate can be defined by the operator. The X-axis and Y-axis of the universal coordinates are specified by the orientation of the electromagnetic field generator device (the Z-axis is perpendicular to the horizontal plane). θ_{xi} represents the angle between the tracker vector and the X-Y plane as projected onto a plane perpendicular to the X-axis, whereas θ_{y_i} is the angle between the tracker vector and the X-Y plane mapped onto a plane perpendicular to the Y-axis. For simplicity, the experiments were performed in a plane perpendicular to the X-axis. Thus we used θ_{xi} as the flexion angle, and to further simplify, we used θ_i instead of θ_{xi}. Therefore, the positions of the tip finger, DIP, and PIP joints could be obtained from the following equations:

$$\begin{aligned} y_{PIP} &= L_1 \cos\theta_1, & z_{PIP} &= L_1 \sin\theta_1 \\ y_{DIP} &= \sum_{n=1}^{2} L_n \cos\theta_n, & z_{DIP} &= \sum_{n=1}^{2} L_n \sin\theta_n \\ y_{tip} &= \sum_{n=1}^{3} L_n \cos\theta_n, & z_{tip} &= \sum_{n=1}^{3} L_n \sin\theta_n \end{aligned} \tag{1}$$

Where L_1 is the length of the proximal phalanx, L_2 is the length of the middle phalanx, and L_3 is the length of the distal phalanx. θ_i $(i = 1, 2, 3)$ is the angle of the electromagnetic tracker (with respect to the horizontal plane) attached to the proximal finger segment, middle finger segment, and distal finger segments respectively. Participants' finger movements were first captured with an NDI Aurora sensor. The raw

data was then segmented into several motion regions. Figure 7(a) represents the angle of the middle finger segment of a participant's finger with respect to the horizontal plane (θ_2), the angle of the proximal finger segment of a participant's finger with respect to the horizontal plane (θ_1), and the angle between middle finger segment and proximal finger segment ($\theta_2 - \theta_1$). As depicted in Fig. 7, the participant performed four tasks, resulting in four segments of raw data from the NDI Aurora sensor.

Participants performed the task at varying speeds. The task in Segment 1, for example, took longer to complete than the task in Segment 2. To normalise the data, it was re-analysed based on task completion rather than time (as illustrated in Fig. 7). Fig. 7(a), (b) shows the flexion angle $\theta_2 - \theta_1$, as well as angular velocity ω_1 (derivatives of $\theta_2 - \theta_1$) in both raw data and fitted curves. To determine the beginning and end point of a segment an angular velocity analysis was conducted. We assumed that if the magnitude of angular velocity was less than $0.1|\omega_{max}|$ then the finger motion could be considered negligible i.e.

if $|\omega_i| < 0.1|\omega_{\max}|$ **then** joint motion is negligible

Here $|\omega_{max}| \cong 128$ deg/s. As a result, we consider 12.8 deg/s as the margin. If $|\omega_i| < 12.8$, then the flexion angle $\theta_2 - \theta_1$ is considered negligible, and the finger is considered to be motionless. If $\omega_i > 12.8$ it is the ascending part of the segment and if $\omega_i < -12.8$, it is the descending part of the segment as shown in Fig. 7. As can be seen, the raw ωi data is not smooth, so to perform the aforementioned analysis we fitted a curve into the raw data (see Fig. 7(b)).

VI. Results

Soft actuators of varying volumes, configurations, and constituent materials are studied and compared in this section. The flexion angles and fluid pressure were recorded as explained in the data capture and data segmentation section. The study results are illustrated in Tables III and IV and Fig. 8. The average pressure generated by actuator i (along with its standard deviation) is designated as P_i, and the mean flexion angle of the prosthetic finger's DIP joint (along with its standard deviation), is represented by ϕ_i. As mentioned in Section IV, three-way ANOVA tests were employed to analyse the experiment results. In the first three-way ANOVA test, the dependent variable was the generated pressure. The statistical analysis revealed significant interactions between configuration and material ($p-value < 0.0001$), configuration and volume ($p - value < 0.0001$), and material and volume ($p - value < 0.0001$). Moreover, the analysis revealed a significant three-way interaction among configuration, material, and volume ($p - value < 0.0001$). These interactions suggest that the effect of each independent variable on the generated pressure depends on the levels of the other independent variables. In the second three-way ANOVA test, the dependent variable was the prosthetic finger's DIP joint flexion angle. The analysis revealed significant interactions between configuration and volume ($p-value < 0.0001$), configuration and material ($p - value < 0.0001$), and material and volume ($p - value < 0.0001$). Additionally, a significant three-way interaction among configuration, material, and volume was observed ($p - value < 0.0001$).

A. Material of soft actuator

The statistical analysis showed that the main effect of the material on both generated pressure and the prosthetic finger's DIP joint flexion angle was significant ($p - value < 0.0001$), i.e. the type of material influences the generated pressure and prosthetic finger's DIP joint flexion angle. To determine which of the three materials produced the highest flexion angle and fluid pressure, we conducted a study using a fixed configuration and volume. The results showed that Ecoflex 00-50, which has the lowest tensile strength of the three materials (315 psi), produced lower pressure and flexion angles than Dragon Skin 30 (with a tensile strength of 500 psi) and Agilus 30 (with a tensile strength of 348-450 psi) across almost all actuators with the fixed configuration and volume ($p-value < 0.0001$). The comparison between Agilus 30 and Dragon Skin 30 reveals that, under the same configuration and volume, Dragon Skin 30 generates higher pressure in nearly all instances (e.g., $P4 > P7 > P1$). However, regarding flexion angles, the values vary, with Agilus 30 achieving higher values in some cases (e.g., $\phi_8 > \phi_5 > \phi_2$) while Dragon Skin 30 excels in others (e.g., $\phi_4 > \phi_7 > \phi_1$), see Tables III and IV. In terms of fabrication, Dragon Skin 30 is manufactured through moulding, which is time-consuming, whereas Agilus 30 is made using a special 3D printing process for soft materials - quicker, but more expensive and less accessible. With pros and cons evident for each material, our recommendation is therefore to keep both Dragon Skin 30, and Agilus 30 open for future applications. Given these findings, it is appropriate to exclude Ecoflex 00-50 from further considerations in the study.

B. Volume of soft actuator

The statistical analysis showed that the main effect of the volume on both generated pressure and the prosthetic finger's DIP joint flexion angle was not significant (p-value = 0.9505, p-value = 0.9163). These suggest that changes in volume do not significantly affect the generated pressure and the prosthetic finger's DIP joint flexion angle.

C. Configuration of soft actuator

The statistical analysis showed that the main effect of configuration on both generated pressure and the prosthetic finger's DIP joint flexion angle was significant ($p - value < 0.0001$), indicating that different configurations lead to statistically significant differences in the generated pressure. To determine which configuration produces the highest pressure and greatest DIP flexion angles, we tested all five configurations, while keeping material and volume fixed. These designs were fabricated in three different materials and two volumes of 1.9 cm³ and 3.1 cm³, as shown in Tables III and IV. The results indicate that Configurations 2 and 3 produced the lowest pressure and flexion angles and can be disregarded from the study.

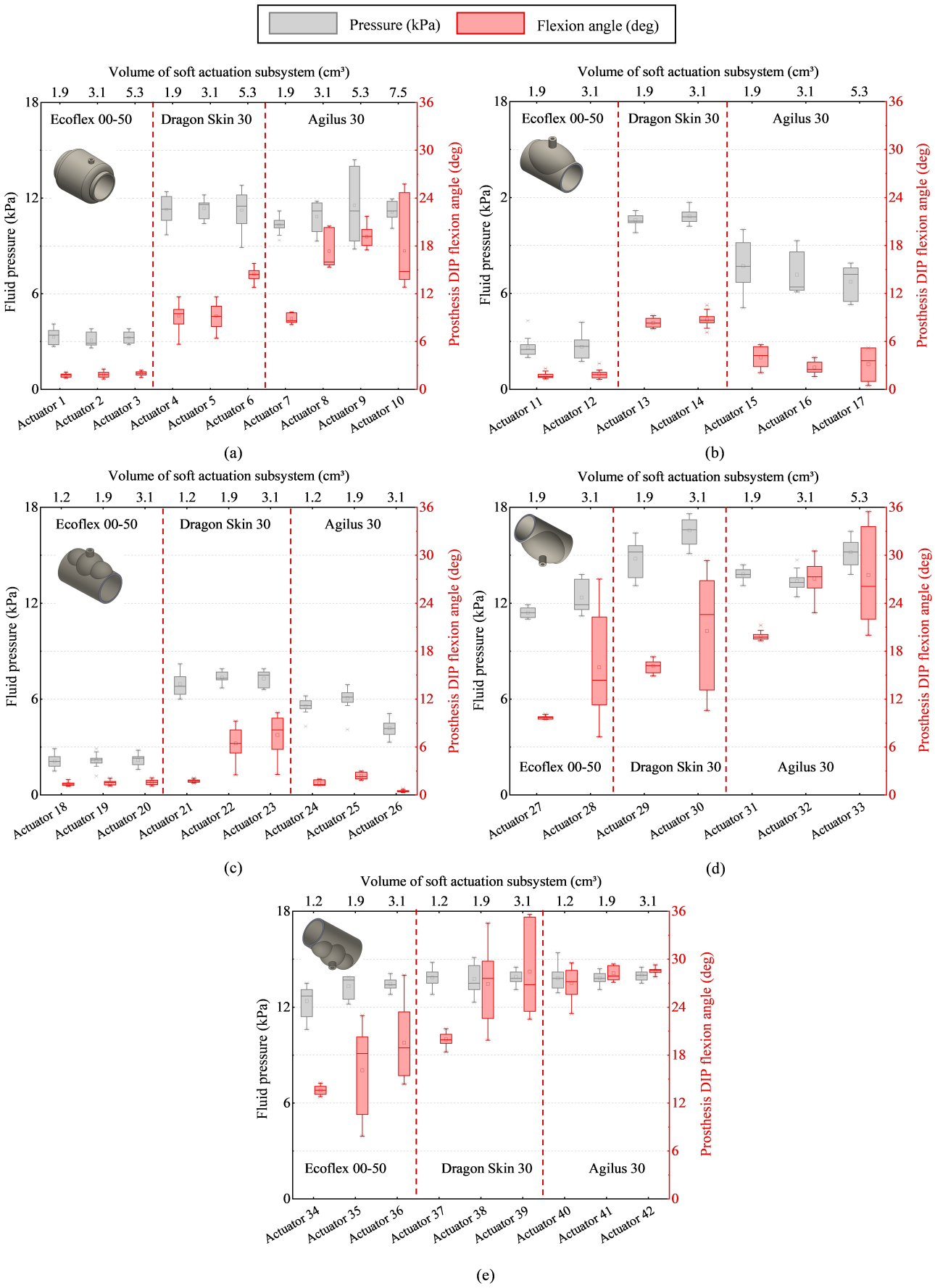

Fig. 8. Showcasing mean values and standard deviations of generated pressure (grey lines) and prosthetic finger DIP joint's flexion angle (red lines) (a) Configuration 1. (b) Configuration 2. (c) Configuration 3. (d) Configuration 4. (e) Configuration 5.

TABLE III
DIP JOINT'S FLEXION ANGLE OF THE PROSTHETIC FINGER.

Shape	Material	Prosthesis DIP flexion angle mean value (SD) [deg]				
		Volume				
		1.2 (cm^3)	1.9 (cm^3)	3.1 (cm^3)	5.3 (cm^3)	7.5 (cm^3)
Configuration 1	Ecoflex 00-50		ϕ_{1^*}=1.75 (0.23)	ϕ_2=1.84 (0.37)	ϕ_3=1.98 (0.27)	
	Dragon Skin 30		ϕ_4=9.20 (1.38)	ϕ_5=9.22 (1.42)	ϕ_6=14.45 (0.99)	
	Agilus 30		ϕ_7=8.88 (0.56)	ϕ_8=17.34 (3.21)	ϕ_9=19.15 (0.59)	ϕ_{10}=17.36 (5.72)
Configuration 2	Ecoflex 00-50		ϕ_{11}=1.72 (0.40)	ϕ_{12}=1.92 (0.51)		
	Dragon Skin 30		ϕ_{13}=8.32 (0.60)	ϕ_{14}=8.73 (0.85)		
	Agilus 30		ϕ_{15}=4.02 (1.34)	ϕ_{16}=2.74 (1.52)	ϕ_{17}=3.16 (1.92)	
Configuration 3	Ecoflex 00-50	ϕ_{18}=1.42 (0.39)	ϕ_{19}=1.52 (0.28)	ϕ_{20}=1.60 (0.32)		
	Dragon Skin 30	ϕ_{21}=1.77 (0.21)	ϕ_{22}=6.43 (1.95)	ϕ_{23}=7.51 (2.22)		
	Agilus 30	ϕ_{24}=1.46 (0.31)	ϕ_{25}=2.36 (0.42)	ϕ_{26}=1.63 (0.23)		
Configuration 4	Ecoflex 00-50		ϕ_{27}=9.72 (0.23)	ϕ_{28}=15.97 (6.02)		
	Dragon Skin 30		ϕ_{29}=16.15 (0.85)	ϕ_{30}=20.51 (6.77)		
	Agilus 30		ϕ_{31}=19.88 (0.61)	ϕ_{32}=27.07 (3.89)	ϕ_{33}=27.52 (6.84)	
Configuration 5	Ecoflex 00-50	ϕ_{34}=13.57 (0.51)	ϕ_{35}=16.08 (5.01)	ϕ_{36}=19.04 (5.45)		
	Dragon Skin 30	ϕ_{37}=19.96 (0.81)	ϕ_{38}=26.91 (4.22)	ϕ_{39}=27.46 (8.66)		
	Agilus 30	ϕ_{40}=27.01 (2.05)	ϕ_{41}=28.26 (0.95)	ϕ_{42}=28.58 (0.44)		

* Identifying numbers for soft actuators.

TABLE IV
GENERATED PRESSURE OF DIFFERENT SOFT ACTUATORS.

Shape	Material	Fluid pressure mean value (SD) [kPa]				
		Volume				
		1.2 (cm^3)	1.9 (cm^3)	3.1 (cm^3)	5.3 (cm^3)	7.5 (cm^3)
Configuration 1	Ecoflex 00-50		P_{1^*}=3.28 (0.46)	P_2=3.09 (0.41)	P_3=3.25 (0.40)	
	Dragon Skin 30		P_4=11.29 (0.76)	P_5=11.35 (0.59)	P_6=11.25 (1.50)	
	Agilus 30		P_7=10.31 (0.60)	P_8= 10.84 (0.93)	P_9=11.54 (2.06)	P_{10}=11.13 (0.65)
Configuration 2	Ecoflex 00-50		P_{11}=2.61 (0.65)	P_{12}=2.67 (0.66)		
	Dragon Skin 30		P_{13}=10.58 (0.82)	P_{14}=10.81 (0.37)		
	Agilus 30		P_{15}=7.71 (1.34)	P_{16}=7.18 (1.70)	P_{17}=6.74 (0.97)	
Configuration 3	Ecoflex 00-50	P_{18}=2.10 (0.62)	P_{19}=2.13 (0.45)	P_{20}=2.17 (0.36)		
	Dragon Skin 30	P_{21}=6.93 (0.85)	P_{22}=7.34 (0.33)	P_{23}=7.29 (0.47)		
	Agilus 30	P_{24}=5.55 (0.42)	P_{25}=6.06 (0.57)	P_{26}=4.17 (0.41)		
Configuration 4	Ecoflex 00-50		P_{27}=11.42 (0.38)	P_{28}=12.35 (0.90)		
	Dragon Skin 30		P_{29}=14.78 (1.23)	P_{30}=16.55 (0.80)		
	Agilus 30		P_{31}=13.82 (0.27)	P_{32}=13.37 (0.71)	P_{33}=15.19 (0.83)	
Configuration 5	Ecoflex 00-50	P_{34}=12.38 (1.18)	P_{35}=13.31 (0.67)	P_{36}=13.44 (0.32)		
	Dragon Skin 30	P_{37}=13.85 (1.08)	P_{38}=13.77 (0.88)	P_{39}=13.89 (0.39)		
	Agilus 30	P_{40}=13.80 (0.84)	P_{41}=13.82 (0.13)	P_{42}=13.98 (0.26)		

* Identifying numbers for soft actuators.

Configurations 4 and 5 produced the highest flexion angles and pressures, while Configuration 1 generated considerable flexion angles and pressure. Although Configurations 4 and 5 produce higher flexion angles and pressures than Configuration 1, their location on the underside of the PIP joint reduces the hand workspace. We suggest considering both Configuration 1 around the finger and Configurations 4 and 5 as design alternatives.

D. Finger movement tracking

For illustrative purposes, we presented data obtained from one participant wearing one of the selected actuators (we selected no. 42 - a Configuration 5 actuator, made of Agilus 30 with a volume of 3.1 cm^3). The flexion angles and the fluid pressure were measured using electromagnetic trackers and a pressure transducer and then segmented and analysed per Section V. Analysing the data against task completion, rather than time, enables us to determine the mean values for each task. Figures 7(c)-(f) illustrate the fluid pressure, participant PIP flexion angle, participant DIP flexion angle, and prosthesis DIP flexion angle, all measured during task completion while the participant wore the soft actuator. The gray lines show the values of pressure and flexion angles in four different segments and the red line shows their mean values. We also measured finger movement participants without the actuator (see Fig. 7(g) and 7(h)). These measurements were then compared to the flexion angles of human fingers while wearing the actuator (i.e. Fig. 7(d) and(e)). We observed that the use of the actuators resulted in a restriction of less than 10% in the movement of a participant's DIP and PIP flexion angles. The mean value of the participants' PIP flexion angle was approximately 100 degrees and the DIP flexion angle was around 60 degrees. The prosthetic DIP flexion angle reached 35 degrees. Figures 7 (c)-(f) also demonstrate that prosthetic DIP flexion dynamics are

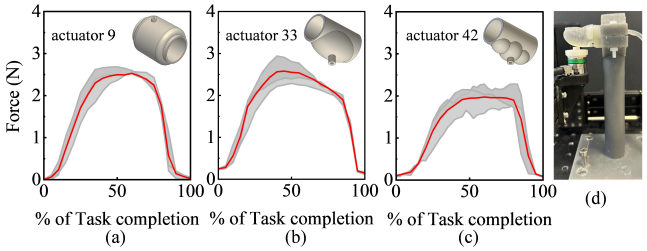

Fig. 9. Force on the fingertip versus task completion (a) for actuator no. 9 (b) actuator no. 33 (c) actuator no. 42 (d) Fingertip's force interface workbench setup

similar to human digit flexion.

E. Fingertip force

Fingertip force assessment was conducted using three soft actuators - no. 9, 33, and 42 - as shown in Fig. 9(a)-(c) respectively. Figure 9 illustrates that actuators 9, 33, and 42 were able to exert fingertip forces of up to 2.3 N, 2.7 N, and 2.9 N respectively.

VII. Discussion

The results of this study indicate that Agilus 30 and Dragon Skin 30 are potentially better options than Ecoflex 00-50. Availability was a key consideration in our recommendation of these materials. Configuration analysis led to the exclusion of Configurations 2 and 3, resulting in our final selection of Configuration 1, Configuration 4, and Configuration 5. Based on the results of the volume test subsection, Configuration 1 with a volume of 5.3 cm^3 (actuator no. 9 in Table IV), Configuration 4 with a volume of 5.3 cm^3 (actuator no. 33 in Table IV), and Configuration 5 with a volume of 3.1 cm^3 (actuator no. 42 in Table IV) were determined to be the best choices. Table VI shows the forces generated in various hand prostheses ranging from 5 to 41 N for body-powered prostheses. The forces provided by hand prostheses encompass grasping, pinching, and fingertip forces. Fine motor tasks typically require fingertip forces of around 2 N [45], [46]. As an example, tapping a computer key generally requires a force ranging from 0.4 to 1.4 N [46]. Gripping a small object such as a pencil requires a force of less than 2 N [47], while the force required for writing varies between individuals, ranging from 0.23 to 7.0 N [45]. By comparing the values listed in Table VI, it can be seen the forces produced by our proposed hydraulic mechanism align with the force requirements for fine motor tasks, affirming their suitability for such applications. It is important to note that the measured force for the proposed finger prosthetic device pertains to one fingertip, whereas the forces reported in Table VI correspond to a hand with multiple fingers.

VIII. Limitations and Future Work

While this study presents significant advancement in the development of a novel body-powered hydraulically-driven prosthetic finger, several limitations and avenues for future research have been identified. Performance optimisation could be achieved by reducing pressure loss from the connecting tubes. As part of our continued research, we will enhance the prosthesis' performance by refining the soft joint mechanism. By refining the soft joint mechanism, the generated force will increase, allowing the execution of more demanding tasks. In addition, further investigations with amputee participants are needed to validate the device's performance and usability within the target user population. In terms of the design of the soft actuator, further work might involve customising its dimensions to suit individual needs. This could be achieved through parametric design processes, enabling the automatic generation of custom-fitting designs tailored to each patient's anatomy.

IX. Conclusions

By focusing on amputations involving the loss of distal and partial middle finger segments, we introduced a novel soft wearable hydraulic mechanism that effectively transmits pressure from the PIP joint of the human finger to the DIP joint of the prosthetic finger. This hydraulic-driven system represents a departure from traditional rigid mechanisms and, in doing so, contributes to the advancement of versatile body-powered prosthetic devices, with potential applications in affordable healthcare solutions. During the study, we examined the design parameters of our soft actuator subsystem to optimise its performance. We investigated aspects such as configuration, fluid chamber placement around the PIP joint, actuator material, and volume. Experimental data collected from able-bodied participants wearing a variety of soft actuators led to the selection of optimal design choices.

Based on statistical analysis, we identified Agilus 30 and Dragon Skin 30 as superior material options, displaying favorable stiffness characteristics as compared to Ecoflex 00-50. Three specific designs (no. 9, 33, and 42) were selected in light of their performance, details of which are presented in Table IV. The experimental results, after normalisation, indicate that the behaviour of the prosthetic finger's distal interphalangeal joint closely resembles that of the human finger's. Although the maximum flexion angle of the prosthetic DIP joint is below its human counterpart, this outcome holds promise as we push forward with further refinement and optimisation of our soft joint design.

References

[1] K. Ziegler-Graham *et al.*, "Estimating the prevalence of limb loss in the united states: 2005 to 2050," *Arch Phys Med Rehabil*, vol. 89, pp. 422–429, 2008.
[2] E. A. Biddiss and T. T. Chau, "Upper limb prosthesis use and abandonment: a survey of the last 25 years," *Prosthet Orthot Int*, vol. 31, pp. 236–257, 2007.
[3] A. Esquenazi, "Amputation rehabilitation and prosthetic restoration. from surgery to community reintegration," *Disabil Rehabil*, vol. 26, pp. 831–836, 2004.
[4] J. T. Le and P. R. Scott-Wyard, "Pediatric limb differences and amputations," *Phys Med Reh Clin*, vol. 26, pp. 95–108, 2015.
[5] C. Lake and R. Dodson, "Progressive upper limb prosthetics," *Phys Med Reh Clin*, vol. 17, pp. 49–72, 2006.
[6] N. T. Kearns *et al.*, "Differences in level of upper limb loss on functional impairment, psychological well-being, and substance use.," *Rehabil Psychol*, vol. 63, p. 141, 2018.

[7] G. B. Silva *et al.*, "Role of arteriovenous vascular loops in microsurgical reconstruction of the extremities," *Acta Ortop Bras*, vol. 26, pp. 127–130, 2018.

[8] E. M. Graham *et al.*, "Restoring form and function to the partial hand amputee: prosthetic options from the fingertip to the palm," *Hand Clin*, vol. 37, pp. 167–187, 2021.

[9] A. Runkel *et al.*, "Risk factors in distal interphalangeal joint arthrodesis in the hand: a retrospective study of 173 cases," *Hand Surg*, vol. 47, no. 9, pp. 907–914, 2022.

[10] H. Chan *et al.*, "Arthroplasty of the distal interphalangeal joint: a review of currently available surgical approaches, implants and complications," *Orthop Surg and Tech*, 2021.

[11] M. Arazpour *et al.*, "The effect of new method of suspension on quality of life, satisfaction, and suspension in patients with finger prostheses," *Prosthet Orthot Int*, vol. 39, pp. 197–203, 2015.

[12] M. C. Goiato *et al.*, "Finger prosthesis: the art of reconstruction," *J Coll Physicians Surg Pak*, vol. 19, pp. 670–671, 2009.

[13] S. L. Carey *et al.*, "Differences in myoelectric and body-powered upper-limb prostheses: Systematic literature review.," *Rehabil Res Dev*, vol. 52, 2015.

[14] A. Goyal and H. Goel, "Prosthetic rehabilitation of a patient with finger amputation using silicone material," *Prosthet Orthot Int*, vol. 39, pp. 333–337, 2015.

[15] J. W. Hung and Y. H. Wu, "Fitting a bilateral transhumeral amputee with utensil prostheses and their functional assessment 10 years later: A case report," *Arch Phys Med Rehab*, vol. 86, pp. 2211–2213, 2005.

[16] M. J. Highsmith *et al.*, "Design and fabrication of a passive-function, cylindrical grasp terminal device," *Prosthet Orthot Int*, vol. 33, pp. 391–398, 2009.

[17] L. Hancock *et al.*, "Cognitive predictors of skilled performance with an advanced upper limb multifunction prosthesis: a preliminary analysis," *Disabil Rehabil*, vol. 12, pp. 504–511, 2017.

[18] E. D. Engeberg and S. Meek, "Improved grasp force sensitivity for prosthetic hands through force-derivative feedback," *IEEE Trans Biomed Eng*, vol. 55, pp. 817–821, 2008.

[19] M. Tavakoli *et al.*, "Anthropomorphic finger for grasping applications: 3d printed endoskeleton in a soft skin," *Int J Adv Manuf Technol*, vol. 91, pp. 2607–2620, 2017.

[20] C. Cipriani *et al.*, "A novel concept for a prosthetic hand with a bidirectional interface: a feasibility study," *IEEE Trans Biomed Eng*, vol. 56, pp. 2739–2743, 2009.

[21] R. Ayub *et al.*, "Evaluation of transradial body-powered prostheses using a robotic simulator," *Prosthet Orthot Int*, vol. 41, pp. 194–200, 2017.

[22] J. A. Doeringer and N. Hogan, "Performance of above elbow body-powered prostheses in visually guided unconstrained motion tasks," *IEEE Trans Biomed Eng*, vol. 42, pp. 621–631, 1995.

[23] K. Berning *et al.*, "Comparison of body-powered voluntary opening and voluntary closing prehensor for activities of daily life," *J Rehabil Res Dev*, vol. 51, pp. 253–61, 2014.

[24] K. D. Gemmell *et al.*, "Investigation of a passive capstan based grasp enhancement feature in a voluntary-closing prosthetic terminal device," in *Int Conf IEEE Eng Med Biol Soc*, pp. 5019–5025, IEEE, 2016.

[25] L. H. Huinink *et al.*, "Learning to use a body-powered prosthesis: changes in functionality and kinematics," *J Neuroeng Rehabil*, vol. 13, pp. 1–12, 2016.

[26] B. D. Veatch, "Joint and digit," Sept. 26 2016. US Patent 15276753.

[27] M. C. Goiato *et al.*, "Implant-retained finger prosthesis with modified retention system," *Prosthet Orthot Int*, vol. 37, pp. 324–328, 2013.

[28] A. Griffart *et al.*, "Arthroplasty of the proximal interphalangeal joint with the tactys® modular prosthesis," *Hand Surg Rehabil*, vol. 38, pp. 179–185, 2019.

[29] G. Faccioli *et al.*, "Prosthesis for metacarpal-phalangeal and interphalangeal joints in hands or feet," Nov. 16 1999. US Patent 5,984,971.

[30] C. Behrend *et al.*, "Update on advances in upper extremity prosthetics," *J Hand Surg*, vol. 36, pp. 1711–1717, 2011.

[31] E. Difonzo *et al.*, "Advances in finger and partial hand prosthetic mechanisms," *Robotics*, vol. 9, p. 80, 2020.

[32] M. Tian *et al.*, "Design and experimental research of pneumatic soft humanoid robot hand," in *Robot Intel Tech Applic*, pp. 469–478, Springer, 2017.

[33] T. Takayama *et al.*, "Assemblable tools for laparoscopic surgery," in *Int Symp Micro-NanoMechatronics Hum Sci*, pp. 59–64, IEEE, 2010.

[34] G. Gu *et al.*, "A soft neuroprosthetic hand providing simultaneous myoelectric control and tactile feedback," *Nat Biomed Eng*, vol. 7, pp. 589–598, 2023.

[35] M. A. Devi *et al.*, "A novel underactuated multi-fingered soft robotic hand for prosthetic application," *Robot Auton Syst*, vol. 100, pp. 267–277, 2018.

[36] J. D. Brown *et al.*, "An empirical evaluation of force feedback in body-powered prostheses," *IEEE Trans Neural Syst Rehabil Eng*, vol. 25, pp. 215–226, 2016.

[37] G. Smit *et al.*, "Efficiency of voluntary opening hand and hook prosthetic devices," *J Rehabil Res Dev*, vol. 49, pp. 523–34, 2012.

[38] S. J. Mirmohammadi *et al.*, "Anthropometric hand dimensions in a population of iranian male workers in 2012," *Int J Occup Saf Ergon*, vol. 22, pp. 125–130, 2016.

[39] X. Yang *et al.*, "Analysis of natural finger-press motions for design of trackball buttons," *Ergonomics*, vol. 62, pp. 767–777, 2019.

[40] L. Marechal *et al.*, "Toward a common framework and database of materials for soft robotics," *Soft robotics*, vol. 8, pp. 284–297, 2021.

[41] J. F. M. Manschot and A. Brakkee, "The measurement and modelling of the mechanical properties of human skin in vivo—i. the measurement," *J biomech*, vol. 19, no. 7, pp. 511–515, 1986.

[42] N. Elango and A. A. M. Faudzi, "A review article: investigations on soft materials for soft robot manipulations," *Int J Adv Manufact Tech*, vol. 80, pp. 1027–1037, 2015.

[43] F. Schmitt *et al.*, "Soft robots manufacturing: A review," *Front Robot AI*, vol. 5, p. 84, 2018.

[44] J. Shi *et al.*, "Stiffness modelling and analysis of soft fluidic-driven robots using lie theory," *Int J Robot Res*, vol. 43, pp. 354–384, 2024.

[45] L. F. Borjón and G. F. Phillips, "Force measurements for tetraplegic writing," in *Int Conf IEEE Eng Med Biol Soc*, vol. 4, pp. 1548–1549, IEEE, 1992.

[46] D. L. Jindrich *et al.*, "Finger joint impedance during tapping on a computer keyswitch," *J Biomech*, vol. 37, pp. 1589–1596, 2004.

[47] G. Obinata *et al.*, "Vision based tactile sensor using transparent elastic fingertip for dexterous handling," in *Mobile Robots: Perception & Navigation*, IntechOpen, 2007.

[48] J. Brooke, "Sus: a "quick and dirty'usability," *Usabil evalu in indust*, vol. 189, pp. 189–194, 1996.

[49] A. Bangor *et al.*, "Determining what individual sus scores mean: Adding an adjective rating scale," *J Usability Stud*, vol. 4, pp. 114–123, 2009.

[50] G. Smit *et al.*, "Efficiency of voluntary closing hand and hook prostheses," *Prosthetics and orthotics international*, vol. 34, pp. 411–427, 2010.

[51] G. Smit *et al.*, "The lightweight delft cylinder hand: first multi-articulating hand that meets the basic user requirements," *IEEE Trans Neural Syst Rehabil Eng*, vol. 23, no. 3, pp. 431–440, 2014.

[52] T. Zhang *et al.*, "Design and functional evaluation of a dexterous myoelectric hand prosthesis with biomimetic tactile sensor," *IEEE Trans Neural Syst Rehabil Eng*, vol. 26, no. 7, pp. 1391–1399, 2018.

[53] J. S. Cuellar *et al.*, "Design of a 3d-printed hand prosthesis featuring articulated bio-inspired fingers," *J Eng in Medicine*, vol. 235, no. 3, pp. 336–345, 2021.

[54] F. Alkhatib *et al.*, "Data for benchmarking low-cost, 3d printed prosthetic hands," *Data in brief*, vol. 25, p. 104163, 2019.

[55] G. Chai *et al.*, "Electrotactile feedback improves grip force control and enables object stiffness recognition while using a myoelectric hand," *IEEE Trans Neural Syst Rehabil Eng*, vol. 30, pp. 1310–1320, 2022.

[56] N. Kerver *et al.*, "The multi-grip and standard myoelectric hand prosthesis compared: does the multi-grip hand live up to its promise?," *J Trans NeuroEng and Rehabil*, vol. 20, no. 1, p. 22, 2023.

Appendix A: Perceived usability of the system

To investigate users' feedback and understand their preferences we conducted experiments using a selected number of actuators. We used the System Usability Scale (SUS) to investigate perceived effectiveness (the user's ability to complete tasks and the quality of task output), efficiency (the resources consumed in task performance), and user satisfaction (subjective reactions to using the system) [48]. We recruited 10 participants and asked them to test each of the selected actuators, repeatedly opening and closing their hands with the actuator connected to the finger mechanism. As many actuators failed to generate sufficient pressure to adequately flex the finger (and therefore being deemed unviable), we limited our SUS assessment to 11 actuators (out of a total of 42). The selection was based on the prosthetic finger's DIP joint flexion angle, denoted as ϕ_i. Actuators were chosen from three distinct groups: Group 1 included those that generated $0 < \phi_i < 10$ degrees, comprising actuators no. 3, 13, 18, 26, and 34; Group 2 comprised those that generated $10 < \phi_i < 20$ degrees (actuators 29, 6, and 8); Group 3 comprised those that generated $20 < \phi_i < 30$ degrees (actuators no. 9, 33, and 42). Participants completed the SUS questionnaire after testing each actuator. SUS assessment utilised the thresholds established by Bangor et al., which classified scores above 50, 68, and 80 as 'OK', 'Good', and 'Excellent', respectively [49]. The SUS scores from our experiments are illustrated in Fig. 10. Actuators no. 42, 33, and 9, which in our experiments produced prosthetic flexion angles of between 19 and 29 degrees, yielded an average SUS score of Mean=81.3 with SD=9.5, which can be considered 'Excellent'. Actuators 6, 8, and 29, with flexion angles of between 9 and 19 degrees, yielded a mean score of 77.2 with SD=11, which is considered 'Good', while actuators no. 3, 13, 17, 18, 26, 34, with flexion angles of between 0 and 9 degrees, produced a SUS mean score 61.6 with an SD of 16.5, which, according to the scale is considered 'OK'. Our choice of actuators in Section VII, i.e. actuators no. 42, 33, and 9, had a SUS mean score of 'Excellent'.

At the conclusion of the SUS assessment, participants were asked to indicate their preferred actuators, materials, configurations, and volumes. Actuator 9 was the most preferred, with a preference rating of 50%, followed by Actuator 33 at 22%. Actuators 42 and 6 had preference rates of 14% each. Regarding material, Agilus 30 was the most preferred, with a preference rating of 86%, while Dragon Skin 30 had a preference rate of 14%. Configuration 1 was the most favored (64%), followed by Configuration 4 (22%) and Configuration 5 (14%). Lastly, in relation to volume, 5.3 cm^3 had a preference rate of 86%, while 3.1 cm^3 had a preference rate of 14%.

TABLE V
PARTICIPANT PREFERENCES FOR ACTUATORS, MATERIALS, CONFIGURATIONS, AND VOLUMES

Category	Selected item	Preference (%)
Actuator	Actuator 6	14%
	Actuator 9	50%
	Actuator 33	22%
	Actuator 42	14%
Material	Agilus 30	86%
	Dragon Skin 30	14%
Configuration	Configuration 1	64%
	Configuration 4	22%
	Configuration 5	14%
Volume	5.3 cm^3	86%
	3.1 cm^3	14%

Appendix B: The measured force produced by various prosthetic hands

TABLE VI
THE MEASURED FORCE PRODUCED BY VARIOUS PROSTHETIC HANDS

Prosthetic Device	Type	Force (N)	Ref.
Hosmer APRL	Body-powered	41	[50]
Hosmer soft hand	Body-powered	5	[50]
Ottobock, 8K24	Body-powered	14	[50]
Delft cylinder hand	Body-powered	30	[51]
Dexterous prosthetic hand	Myoelectric	8-12	[52]
RSL stepper	Myoelectric	3-9	[37]
Ottobock VO hand	Myoelectric	9-12	[37]
Delft 3-D printed prosthetic hand	Body-powered	16	[53]
Qatar University 3D printed prosthetic hand	Body-powered	6	[54]
Shanghai Jiao Tong university hand	Myoelectric	16	[55]
i-limb prosthetic hand	Myoelectric	46-191	[56]
Bebionic prosthetic hand	Myoelectric	26-140	[56]
Vincent prosthetic hand	Myoelectric	12-44	[56]

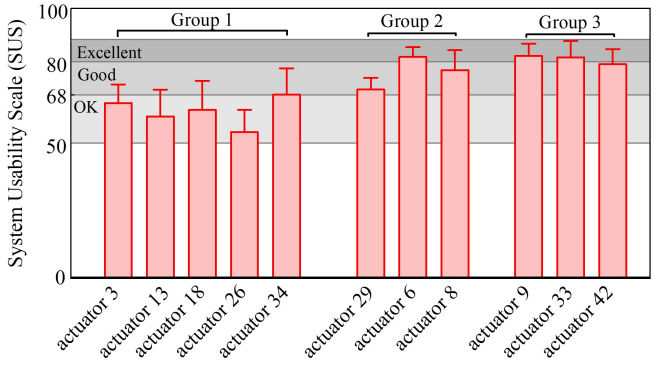

Fig. 10. Average and standard deviation of SUS scores across different actuators